Supplemental Material

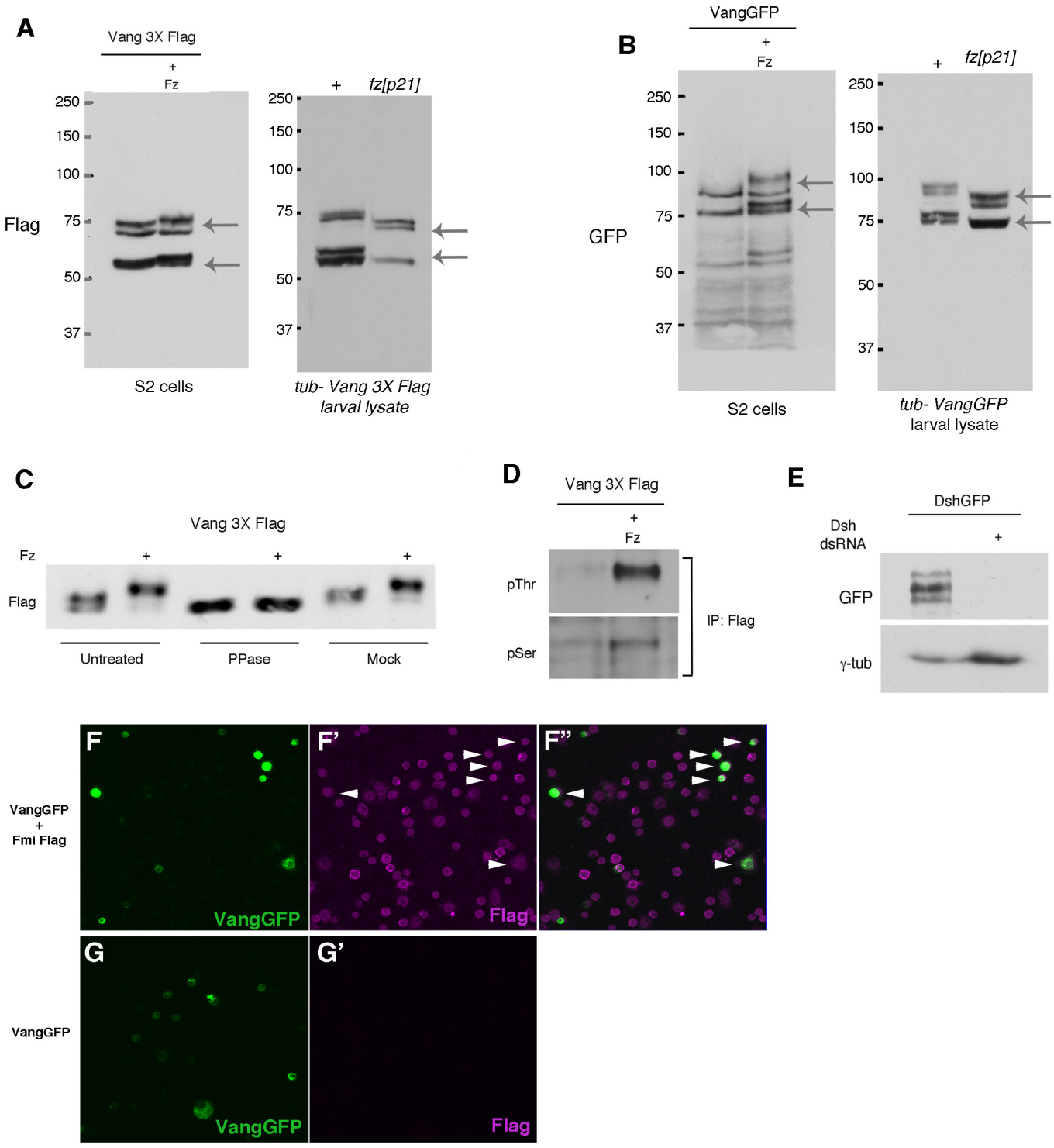

Figure S1 (related to Figure 1). Fz induced Vang band shift is sensitive to phosphatase treatment and Fz induces hyperphosphorylation on Vang serines and threonines in a Dsh independent manner.

(A) Co-transfection of Fz causes a shift in the upper band of the Vang3XFlag doublet in S2 cells (left panel). In a *fz*^{p21} mutant (labeled as *fz[p21]*), the Vang3XFlag band does not display a shift as compared

to the wild-type lysate (right panel). We consistently observe the full-length 3xFlag tagged protein at ~75kDa (upper gray arrow) as well as a ~55kDa breakdown product (lower gray arrow). For the sake of simplicity, we only show data from the full-length protein in the remainder of this work, as there is no evidence for a biological function of any of the breakdown products. In S2 cells we could generally detect a doublet (with some constitutive phosphorylation independent of Fz), whereas *in vivo* samples appeared as a single band in lysates from *fz-/-* animals or phosphatase treated wild-type samples, compared to a single slower migrating band in untreated samples.

(B) Co-transfection of Fz causes a shift in the upper band of the VangGFP doublet in S2 cells (left panel). In a fz^{p21} mutant (labeled as *fz[p21]*), the VangGFP band does not display a shift as compared to the wild-type lysate (right panel). We consistently observe the full-length GFP tagged protein at ~95kDa (upper gray arrow) as well as a ~75kDa breakdown product (lower gray arrow) as well as occasional smaller breakdown products.

(C) Treatment of cell lysates with lambda protein phosphatase inhibits the Vang band shift event, indicating that it is due to phosphorylation.

(D) Co-transfection of Fz causes hyperphosphorylation of Vang on serine and threoine residues. Precipitate from cells transfected with Vang3XFlag shows weak signals with pThr and pSer antibodies, indicative of basal phosphorylatione events. Precipitate from cells co-transfected with Vang3XFlag and Fz shows stronger pThr and pSer signals, representing an increase in phosphorylation events.

(E) Western blot of S2 cells transfected with DshGFP; sample in right lane treated with Dsh dsRNA (same as used in Fig. 1G) prior to transfection. Dsh dsRNA efficiently reduces levels of Dsh protein.

(F-G') Fmi is expressed in S2 cells co-transfected with VangGFP and Fmi, as detected by Fmi antibody staining (F'). Compare to cells transfected with only VangGFP in G and G'. Basically all cells that transfected with Vang also were transfected with Fmi.

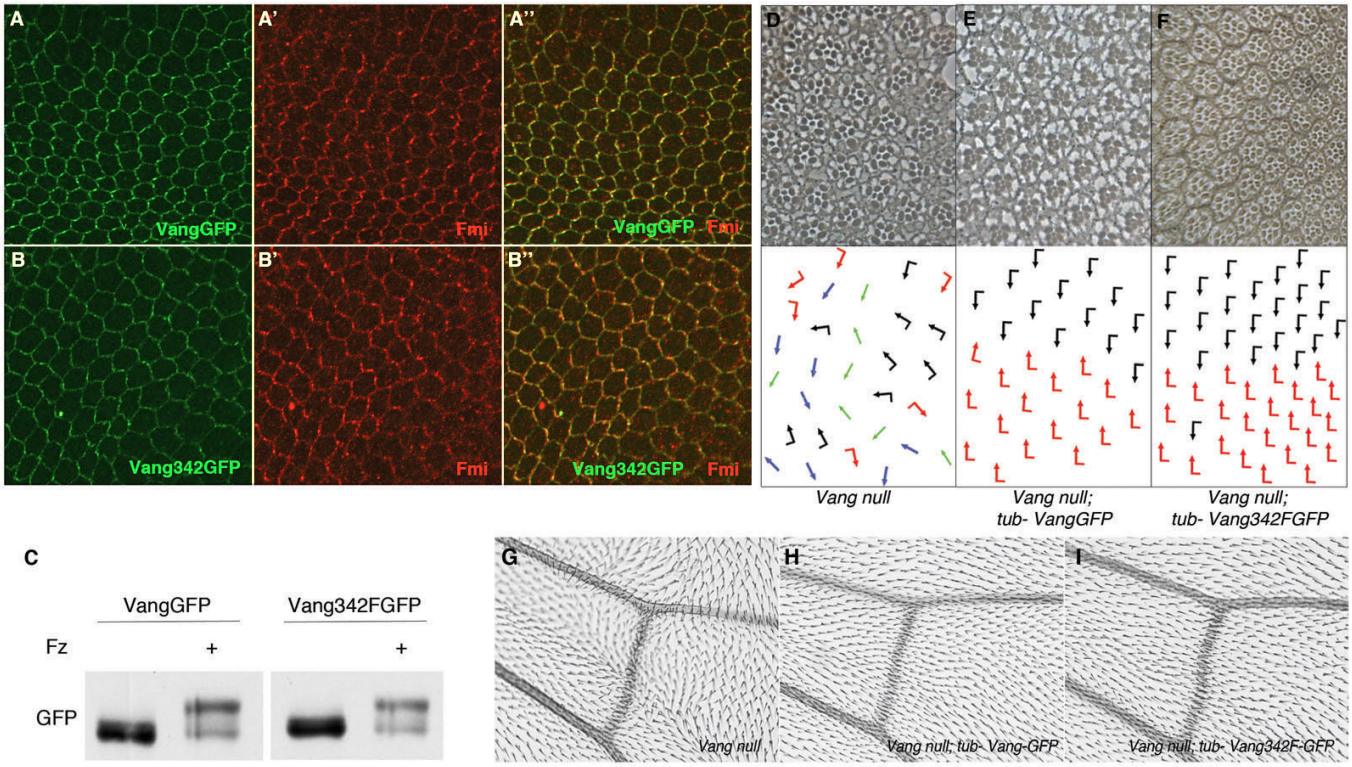

Figure S2 (related to Figure 2). VangY342 is not required for Vang membrane localization or function.

(A-B) Pupal wings (at 32 hr APF), stained for GFP, detecting VangGFP and Fmi (red). (A) *tub-Vang-GFP* expressed in a *Vang* null mutant background localizes like wild-type Vang to the proximal membrane region within the proximo-distal axis, overlapping with Fmi (A', A''). (B) *tub-Vang342F-GFP* expressed in a *Vang* null mutant also localizes to the proximal cell border, overlapping with Fmi (B', B'').

(C) The Vang342FGFP mutant undergoes the phosphorylation induced band shift identical to wild-type Vang, upon co-transfection with Fz in S2 cells.

(D-I) Vang341 does not rescue the *Vang*-/- mutant phenotypes.

(D-F) Tangential eye sections of indicated genotypes, showing region flanking the equator (D/V midline; anterior is left and dorsal is up); bottom panels show schematics of ommatidial orientations. Black and red arrows represent dorsal and ventral chirality; green arrows: R3/R3 symmetrical clusters; blue arrows: R4/R4 symmetrical clusters. (D) *Vang*-/- mutant exhibits chirality defects, including symmetrical ommatidia, and rotation defects (E) Expression of *tub-Vang-GFP* fully rescues the *Vang* null mutant phenotype, restoring mirror image ommatidial orientation across the equator. (F) *tub-Vang342F-GFP* rescues nearly all of the *Vang*-/- polarity defects.

(G-I) High magnification of adult wings, near intersection of posterior cross-vein with L4 and L5 veins; proximal is to the left and anterior is up. (G) *Vang* null mutants display misoriented hairs and cells containing multiple cellular hairs. (H) *tub-Vang-GFP* expression rescues the *Vang-/-* PCP defects (hair orientation and multiple cellular hairs). (I) *tub-Vang342F-GFP* also rescues defects in *Vang-/-* wings.

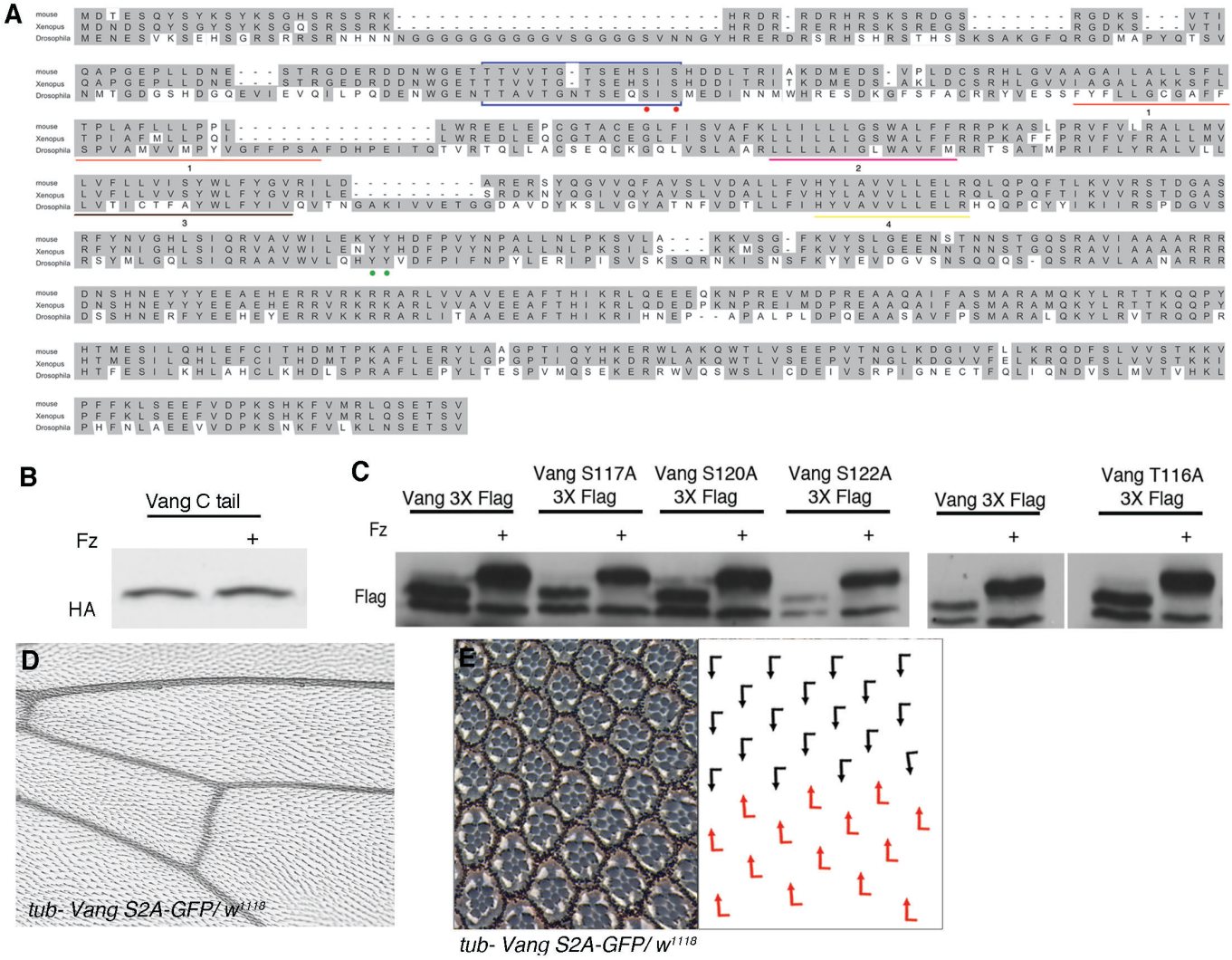

Figure S3 (related to Figure 3). Vang S120/122 are sufficient for the Fz induced band shift and *tub-VangS2A-GFP* expression does not cause gain-of-function phenotypes.

(A) Sequence alignment of Vang/Vangl2 proteins in three species. Mouse Vangl2, Xenopus Vang and Drosophila Vang are compared with the MacVector program. Transmembrane domains are underlined. Blue brackets represent the conserved N-terminal S/T cluster with red dots identifying S120 and S122. Green dots label Y341 and Y342.

(B) Vang constructs containing only the intracellular C-terminal tail (Vang C-tail) do not undergo a band shift when co-transfected with Fz into S2 cells, implying that the phosphorylated residues are not contained within these constructs.

(C) Mutation of individual Vang serines and threonines within the conserved cluster (including S120 and S122) does not affect the Fz induced band shift in cells. S120 and S122 are equivalent and sufficient for the phosphorylation induced band shift event.

(D) High magnification of adult wing; proximal is to the left and anterior is up. Expression of *tub-VangS2A-GFP* in a wild-type (w^{1118}) background does not induce hair reorientation or multiple cellular hairs in the wing.

(E) Tangential eye sections of indicated genotypes, showing region flanking the equator (D/V midline; anterior is left and dorsal is up); bottom panel shows schematics of ommatidial orientations. Black and red arrows represent dorsal and ventral chirality. Expression of *tub-VangS2A-GFP* in a wild-type (w^{1118}) background does not induce polarity defects.

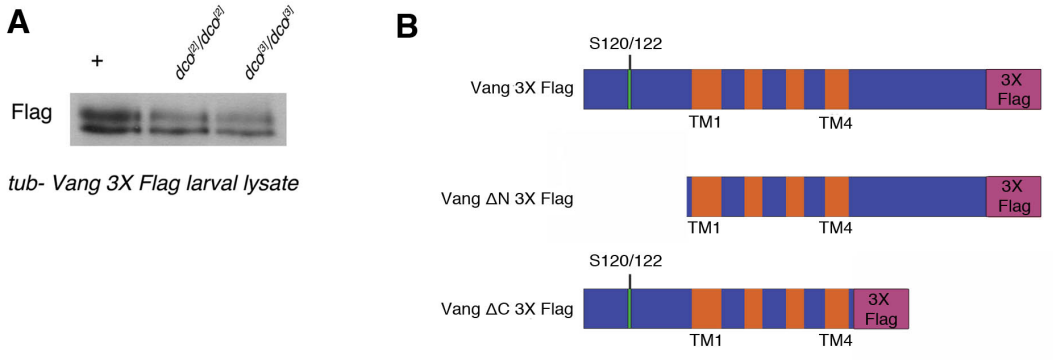

Figure S5 (related to Figure 5). Vang phosphorylation is not affected in hypomorphic *dco* mutants *in vivo*.

(A) In both *dco*^{2} and *dco*^{3} homozygous mutant larval lysate, the band shift of Vang3XFlag was not significantly affected compared to *tub-Vang3XFlag/+* lysate.

(B) Schematic of Vang truncation constructs used in co-immunoprecipitation experiments with Dco. Transmembrane domains are shown in orange. Serines 120/122 are represented by the green bar and the C-terminal 3XFlag tag is shown in pink.

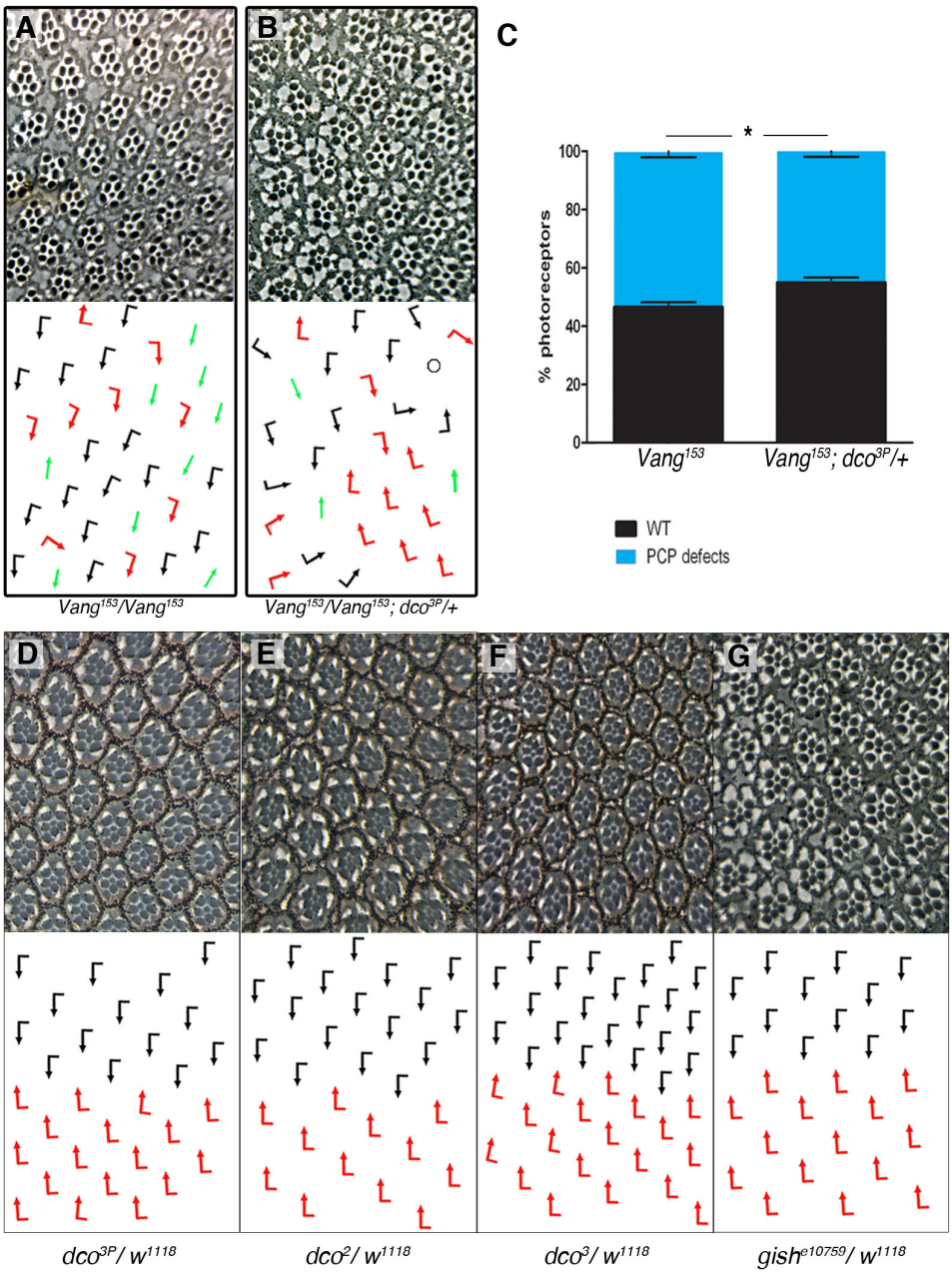

Figure S6 (related to Fugure 6). *dco-/+* modifies a *Vang* loss-of-function phenotype and heterozygous CK1ε/*dco* chromosomes have no PCP phenotypes in an otherwise wild-type background.

(A-C) Homozygous hypomorphic *Vang* loss-of-function allele (*Vang*^{153}) displays symmetrical clusters, chirality and rotation defects (A), which are suppressed (B) upon removing one copy of *dco* (*dco*-/+ with null allele). (C) Quantification of PCP defects observed in genotypes in A-C: % of defects shown in blue (*p<0.05 with student's *t*-test, n=334-396 from 3 independent eyes for each genotype; error bars are S.D) (D-F) Tangential eye sections of indicated genotypes, showing region flanking the equator (D/V midline; anterior is left and dorsal is up); bottom panel shows schematics of ommatidial orientations. Black and red arrows represent dorsal and ventral chirality.